Showcasing research from Xingfu Tang's Laboratory, Department of Environmental Science and Engineering, Fudan University, Shanghai, China.

Fabrication, characterization, and stability of supported single-atom catalysts

Supported single-atom catalysts (SACs) have attracted great attention due to their maximum atom efficiency and unprecedented catalytic activity. Recent progress in the fabrication, characterization, and stability of SACs is outlined and electronic metal–support interactions are proposed as the key to the development of stable SACs.

As featured in:

See Xingfu Tang *et al.*, *Catal. Sci. Technol.*, 2017, **7**, 4250.

ROYAL SOCIETY OF CHEMISTRY

rsc.li/catalysis

Registered charity number: 207890

Catalysis Science & Technology

MINIREVIEW

View Article Online
View Journal | View Issue

Cite this: *Catal. Sci. Technol.*, 2017, 7, 4250

Fabrication, characterization, and stability of supported single-atom catalysts

Yaxin Chen, [a] Zhiwei Huang,[a] Zhen Ma, [a] Jianmin Chen[a] and Xingfu Tang *[ab]

Received 12th April 2017,
Accepted 6th July 2017

DOI: 10.1039/c7cy00723j

rsc.li/catalysis

Supported single-atom catalysts (SACs) and their catalysis have become a hot topic recently, because the dispersion of isolated metal atoms on support surfaces can maximize the atomic efficiency/economy of noble metals and the resulting SACs often possess unprecedented catalytic activity. More importantly, with the development of SACs, it is relatively easy for us to identify the nature of catalytically active sites on these catalysts and establish intrinsic reaction mechanisms. However, it is still a great challenge to develop thermally and chemically stable SACs by a relatively easy method, which is also the case for the characterization of these catalysts because that would need higher resolution and precision. In this minireview, we generalize the advantages of SACs, outline the recent progress of the fabrication, characterization, and stability of SACs, and propose that electronic metal–support interactions are key to the development of stable SACs with pronounced catalytic activity. Some directions for future research are briefly discussed.

1. Introduction

Traditional supported metal catalysts are portrayed by the dispersion of metal nanoparticles (NPs) on the support, whereas single-atom catalysts (SACs) are a class of unconventional catalysts where bare metal atoms are atomically dispersed or anchored on the support.[1–6] In the late 1980s, Thomas defined a new class of catalysts as uniform heterogeneous catalysts.[7] Owing to the development of new and sophisticated characterization techniques/instruments in recent decades, one can "see" single metal atoms with these tools. Thomas *et al.* reviewed the relevant progress till 2005, including a work on single Pd atoms supported on thin MgO films,[8] and renamed this class of catalysts as single-site heterogeneous catalysts (SSHCs).[1] He also categorized SSHCs into four subclasses, one of which includes individual isolated atoms anchored to supports. In 2005, Böhme *et al.* also proposed the conception of single-site catalysis in gas-phase experiments.[9] In 2011, Qiao *et al.*[10] observed single Pt atoms anchored on FeO_x surfaces (Fig. 1) by using high-resolution high-angle annular dark-field scanning transmission electron microscopy (HAADF-STEM), and they coined a new concept of single-atom catalysis, thus provoking a hot debate on whether single atoms alone can act as active sites in heterogeneous catalysis.[11] In 2013, Yang *et al.* generalized the concept and examples of "single-atom catalysts".[3] From that on, more and more articles on SACs have been published. SACs have attracted much attention due to the following aspects.

1.1. Maximum atom efficiency

Noble metals, widely used as catalyst components, are expensive and of limited supply. Thus, enormous efforts have been devoted to reducing the consumption of noble metals. In principle, the catalytically active sites (CASs) of supported noble metal catalysts are either the perimeter atoms of metal NPs in contact with supports or exposed surface atoms of metal NPs,[12–15] whereas the metal atoms inside NPs are often not used for surface catalysis. Thus, the most effective way to make use of each metal atom of supported metal catalysts is to downsize metal NPs to well-defined and atomically distributed metal active centers, *i.e.*, SACs.

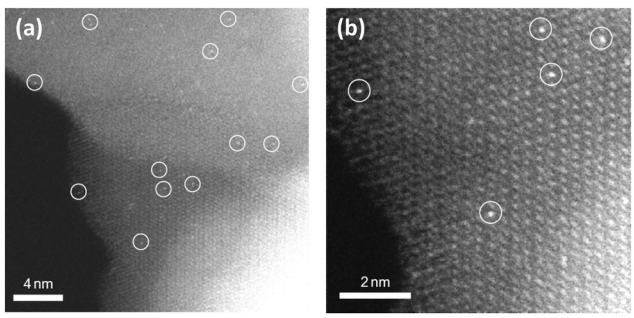

Fig. 1 HAADF-STEM images of Pt_1/FeO_x. Pt single atoms (white circles) are uniformly dispersed on the FeO_x support (a) and occupy exactly the positions of the Fe atoms (b). Reproduced with permission from ref. 10.

[a] *Institute of Atmospheric Sciences, Shanghai Key Laboratory of Atmospheric Particle Pollution & Prevention (LAP[3]), Department of Environmental Science & Engineering, Fudan University, Shanghai 200433, China.*
E-mail: tangxf@fudan.edu.cn
[b] *Jiangsu Collaborative Innovation Center of Atmospheric Environment and Equipment Technology (CICAEET), Nanjing University of Information Science & Technology, Nanjing, 210044, China*

1.2. Unique catalytic properties

In recent years, SACs have been widely used in catalytic oxidation,[10,15–22] hydrogenation,[23–26] water-gas-shift (WGS),[4,27–29] and electrocatalysis,[30–33] showing improved catalytic activity and selectivity compared with supported metal NPs. For example, we prepared single-atom Ag chains (Ag–HMO) from Ag NPs supported on hollandite-type manganese oxide (HMO) nanorods (Ag/HMO), and found that the TOF of Ag–HMO (0.035 s^{-1}) in the HCHO oxidation was much higher than that of Ag/HMO (0.005 s^{-1}) at 80 °C.[34] Flytzani-Stephanopoulos's group discovered that both positively charged Pt and Au single atoms supported on appropriate oxides are the active species for the WGS reaction.[28,29,35] The isolated bimetallic Rh_1Co_3 sites of Rh_1Co_3/CoO exhibited outstanding catalytic performance in terms of quite high catalytic activity and 100% selectivity for the reduction of NO to N_2 at low temperature.[36] Wang *et al.* also developed CoO-supported Rh single-atom catalysts with remarkable activity and selectivity towards propene hydroformylation.[37] A single-atom Pd_1/graphene catalyst showed about 100% selectivity to butenes in the selective hydrogenation of 1,3-butadiene at a 95% conversion, whereas on a commercial Pd/carbon catalyst, the selectivity to all butenes decreased dramatically when the 1,3-butadiene conversion was above 70%.[26]

1.3. Identification of catalytically active sites

Since the introduction of the concept of CASs by Taylor in 1925,[38] great efforts have been devoted to the identification of CASs. A thorough understanding of the nature of CASs may be helpful for improving existing catalysts and designing superior new catalysts.[39–41] However, the precise identification of CASs is extremely challenging, especially for supported metal NP catalysts, due to the quantum size effect[42–44] and the structure-sensitive geometric effect.[45,46] Fujitani *et al.* found that the CASs of Au/TiO_2 for CO oxidation are temperature-dependent; at low reaction temperatures the CASs are only located at the perimeter interfaces of the Au NPs contacted with TiO_2 support, whereas at high temperatures all the surface Au atoms can act as CASs.[12] Ertl's group reported that active metal surfaces often oscillate during the real catalytic oxidation,[47] meaning that CASs can be changeable. Therefore, it is a formidable task to identify the CASs of supported metal NP catalysts.

On the contrary, it is much easier for us to identify the CASs of SACs because the single metal atoms with their immediate neighbouring atoms of the support surfaces are usually CASs. For example, Yang *et al.*[48] reported that at higher gold loadings on titania, nanoparticles formed but gave no further enhancement to the activity. The removal of this "excess" gold leaves the activity intact. Hence, the atomically dispersed gold species with surrounding extra surface –OH groups are the active sites for the WGS reaction. Similar results were also reported in other reactions.[49,50] We synthesized two thermally stable SACs, in which single Ag atoms are anchored at the {001} top facets of HMO by different methods, and we found that the higher depletion of the 4d electronic states of the Ag atoms caused stronger electronic metal–support interactions, leading to easier reducibility and higher catalytic activity (Fig. 2).[51] In our recent work, single-atom sodium and silver catalysts were also used to differentiate the function of alkalis from that of noble metals under identical conditions.[52] Wang *et al.* also established a quantitative correlation between the catalytic performance and metal–support interactions by using Rh_1/VO_2 single-atom catalysts for NH_3BH_3 hydrolysis to generate H_2.[53]

1.4. Establishment of intrinsic reaction mechanisms

As for traditional noble metal NP catalysts, it is extremely difficult to establish an intrinsic reaction mechanism even for a simple model reaction such as CO oxidation. As a consequence, density functional theory (DFT) calculations have played a major role in understanding the specific catalytic reaction mechanisms.[10,18,30,34,54–57] Because single metal atoms act as CASs of SACs, the establishment of intrinsic reaction mechanisms (by using experimental data and DFT calculations) becomes significantly simplified compared with those for metal NP and cluster catalysts. For example, the catalytic mechanisms of CO oxidation on Ir_1/FeO_x or Pt_1/FeO_x catalysts

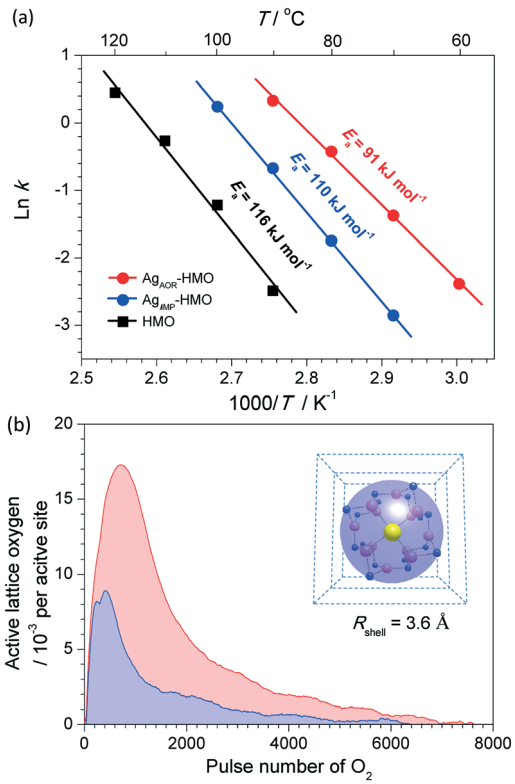

Fig. 2 (a) Arrhenius plots for the reaction rate constants (k) for the HCHO oxidation over the catalysts with the corresponding E_a values. (b) TAP results of Ag_{AOR}–HMO at 70 °C (blue shade) and 100 °C (red and blue shades) using a CO probe. The inset model shows twelve lattice oxygen atoms (pink) within a shell with a radius of approximately 3.6 Å (R_{shell}) of the CAS (yellow) at 70 °C. Mn atoms are depicted as blue balls. Reprinted with permission form ref. 51.

were proposed by using DFT calculations and were further confirmed by experimental results.[10,54] The theoretical investigation helps to understand the differences in the reaction rates between Ir_1/FeO_x or Pt_1/FeO_x for CO oxidation. The mechanisms of other sophisticated reactions such as oxygen reduction reaction[18] and benzene oxidation[30] over SACs were also calculated by DFT.

Although supported single-atom catalysts have demonstrated attractive performance, three dominant challenges remain, including: (i) controllable and facile synthesis of SACs with finely and densely dispersed single atoms; (ii) characterization of SACs, especially *via in situ* techniques; (iii) robust stabilization of single atoms on supports. Below we primarily focus on the recent advances in addressing these three challenges.

2. Fabrication of single-atom catalysts

A prerequisite for studying catalytic properties of SACs is to disperse isolated single metal atoms onto appropriate support surfaces. Methods used for the fabrication of SACs include high-vacuum physical deposition techniques (*e.g.*, a mass-selected soft-landing method[58–60] and an atomic layer deposition method[31]) and wet-chemical routes.[10,19–23,25,29,30,34,61–66] Vacuum deposition of single atoms is easier to control and can provide desirable model catalysts for fundamental studies of metal–support interactions and the particle size effect. However, it may not be possible, at least at the moment, to use this technique to produce commercial catalysts for industrial applications due to the high cost and low yield.[3,5,6] So far, wet-chemical routes have been mainly used to synthesize SACs because this method does not require specialized equipment and can be conveniently practiced. For example, Zhang's group has successfully prepared a series of SACs by coprecipitation, in which single atoms can be Pt or Ir.[10,61,62] Single-atom Pt catalysts based on different supports were also synthesized by impregnation.[26,30,55] A facile adsorption method was also used for the synthesis of single-atom catalysts.[63–66] Different from the usual strategy using the metal monomer as precursors, we synthesized single-Ag-atom catalysts, starting from Ag NPs supported on HMO.[15,19,22,34,51] Upon heating, the Ag NPs on HMO can be dispersed to form single Ag atoms. Although all the wet-chemical routs are convenient compared to high-vacuum physical deposition techniques, different kinds of wet-chemical routs have its own disadvantages. For example, some metal atoms can be buried at the interfacial regions of the support agglomerates and within the bulk of the support crystallites for the coprecipitation method. The wet impregnation method may not be appropriate for synthesizing high metal loading SACs.[6]

2.1. Three kinds of surface sites for anchoring single metal atoms

It is challenging to fabricate SACs with isolated single atoms finely, densely, and tightly anchored to supports. Due to the huge surface-free-energy of single atoms, the aggregation of single atoms during the preparation of catalysts seems to be inevitable, especially when high surface-loading densities of single atoms are desired.[16,23,25,55,64] In addition, SACs are often unstable due to sintering during catalytic reactions, resulting in the loss of activity or selectivity.[3,67] Despite extraordinary difficulties, the fabrication of SACs is feasible depending on the nature of anchoring sites on supports' surfaces.

There are generally three kinds of anchoring sites on the basis of their different structural properties: (i) support surfaces with unsaturated coordinated atoms.[67] Kwak *et al.* reported that Pt atoms bound to unsaturated coordinate Al^{3+} sites on the support by a binding-driven method to achieve a SAC.[67] (ii) Support surfaces with defects.[10] A SAC that Pt atoms are anchored at detects of iron oxide was synthesized.[10] Isolated Au atoms dispersed on the surface of CeO_2 and FeO_x by occupying the surface vacancy sites were proved to be extremely stable for CO oxidation in a wide temperature range.[64,65] (iii) Support surfaces with excess O atoms to form size-suitable hollow sites. Hackett *et al.* synthesized single-site Pd/Al_2O_3 catalysts by stabilizing Pd atoms in a four-coordinate, pseudo-square-planar geometry.[16] A stable Pt_1 SAC based on phosphomolybdic acid (PMA)-modified active carbon was also developed by anchoring Pt on the four-fold hollow sites on PMA.[25] However, only a minority of supports' surfaces has a fairly strong affinity for mobile single atoms, leading to a remarkably low metal loading of 1 wt% or below with respect to supports,[10,67] which causes a relatively low surface concentration of CASs (Fig. 1). Thus, the key to synthesizing stable SACs with high density is to increase the density and capability of anchoring sites.

2.2. Strategies to increase the density of surface single metal atoms

Considering the three kinds of anchoring sites, it is relatively easy to increase the density and to adjust the nature of the oxygen cavities. There are two strategies to solve this problem: one way is to find a support with high-density anchoring sites. Our previous work showed that HMO is a desirable support. Terminated oxygen atoms of the HMO(110) or (001) surfaces serving as suitable cavities could anchor individual metal atoms (such as Ag) with a proper diameter, and the HMO tunnels could also encapsulate individual Ag atoms.[34,51] Therefore, both surfaces and tunnels could densely accommodate single Ag atoms.[51] A catalyst with a high Ag loading of 10 wt% was successfully synthesized. The other way is to downsize metal oxide supports because nanostructured oxide supports have high surface areas and high intensity of defect sites, which played as the anchoring sites of single metal atom. After anchoring the metal atom, energy of the system of the supported single-atom catalyst will decrease according to the DFT calculation.[68] In our recent studies, HMO NPs with potassium-filled pores were synthesized that allows noble metal atoms to be exposed only on

abundant five-fold oxygen-terminated cavities to form highly dense CASs, and the density of single silver atoms on HMO surface was found to arrive at ~2.5 Ag atoms nm^{-2} (Fig. 3), presumably the highest density of dispersed single atoms among the reported SACs.[15,19,69] Dvořák *et al.* found single Pt^{2+} ions are stabilized at ceria step edges in planar PtO_4 moieties, and nanostructured oxide supports may be helpful to increase the loading of monodispersed Pt^{2+} ions.[68] Therefore, nanostructured supports with high-density surface anchoring sites are needed for fabricating SACs with high-density CASs.

3. Characterization of single-atom catalysts

After the fabrication of supposed SACs, it is necessary to characterize them to confirm the existence of only single metal atoms and determine the structure of the CASs. However, that is not an easy task because high spatial resolution is needed to determine single atoms with several-angstrom sizes. Nowadays, sophisticated characterization tools used for that purpose include electron microscopy,[10,16,18,23,24,29,32,35,51,55,68–71] especially scanning tunneling microscopy (STM) and HAADF-STEM, as well as spectroscopic techniques,[10,15–24,34,51,67,70] including X-ray absorption spectroscopy covering extended X-ray absorption fine structure (EXAFS), X-ray absorption near edge structure spectroscopies, and infrared (IR) spectroscopy. Below we discuss the application and challenge of these technologies.

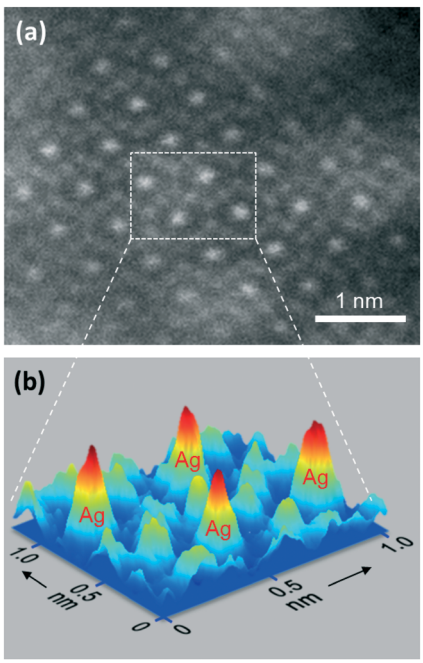

Fig. 3 Imaging of the isolated Ag atoms on the HMO surface. (a) Aberration-corrected HAADF-STEM image of Ag_1/HMO. (b) Three-dimensional projected image of the dash rectangle in panel (a), showing the difference of contrast between Ag, Mn and the background (each peak corresponds to an atom, and the height/intensity of the peaks is dependent on the atomic STEM contrast; arbitrary colors). Reprinted with permission from ref. 69.

3.1. Electron microscopy approach

With the improved resolution on the sub-angstrom scale, electron microscopy has become the most convincing and intuitive approach to evaluate the quality of supported metal catalysts because it can directly image the single metal atoms dispersed on supports, and thus one can identify the location of the single metal atoms with respect to the surface structures of supports and determine the spatial distribution of single metal atoms.[72,73] In particular, HAADF-STEM takes advantage of the Rutherford scattering of electrons to detect heavy atoms on light elements of supports.[74] Wei *et al.* distinguished single metal atoms and subnanometre clusters with a two-dimensional raft-like morphology based on the brightness variations and intensities.[23] Other single metal atoms, such as Pd, Au, Ag, and Fe have been also imaged by HAADF-STEM.[18,25,35,69] However, HAADF-STEM cannot distinguish single metal atoms from supports when their atomic numbers are close. Besides HAADF-STEM, STM can provide both the atomic and electronic structure information of single metal atoms only when the underlying supports are conductive. For example, Deng *et al.* used low-temperature STM images combined with STM simulation to confirm that a FeN_4 center is embedded in the graphene matrix and the iron center significantly modified the density of states of adjacent atoms (Fig. 4).[18]

Although environmental STEM has been developed rapidly in recent years, it is challenging to observe the electronic states of single metal atoms under the reaction environment due to the limitation of the technology, oscillation of

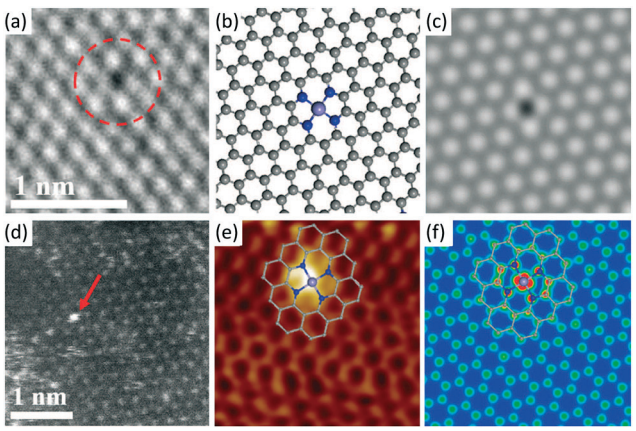

Fig. 4 (a) High-resolution transmission electron microscopy (HRTEM) images of FeN_4/GN-2.7. (b and c) Atomic models (b) and the corresponding simulated HRTEM images (c) for the structures in (a), where the FeN_4/GN structures have been optimized. (d) HAADF-STEM images of FeN_4/GN-2.7. (e) Low-temperature scanning tunneling microscopy (LS-STM) image of FeN_4/GN-2.7, measured at a bias of 1.0 V and a current of 0.3 nA (2 nm × 2 nm). (f) Simulated STM image for (e). The inserted schematic structures represent the structure of the graphene-embedded FeN_4. Reprinted with permission from ref. 18.

catalysts or damage under the high-energy beam or probe current.[75] Hence, it is extremely desirable to develop an almost undamaging electronic imaging technology for *in situ* investigations of structures and chemical behaviors of single atoms in real reaction environments.

3.2. Spectroscopic techniques

EXAFS spectroscopy has been extensively used to characterize the nature of supported metal NPs.[10,15,16,18–24,34,51,70] EXAFS spectra arise due to the interference effects between the outgoing wave and the backscattered wave produced by the surrounding atoms around the core.[76] From the analysis of EXAFS data, information about the local coordination number, interatomic distances, structural disorder, and kind of neighboring atoms at a given distance can be extracted.[76] The parameters primarily reflecting sizes and shapes of metal particles are the average coordination number which can be determined, in principle, up to the fifth coordination shell around the absorber atoms.[77] Thus, if an accurate description of the relation between the particle size/shape and the average coordination number are known, one can estimate the particle geometry. For SACs, the metal–metal bonds should be absent in their EXAFS spectra. In our previous work, EXAFS spectroscopy was successfully applied to evaluate the sizes of supported Ag NPs and determine the structures of the anchoring sites of single Ag atoms (Fig. 5).[15,34,69] The Ag–Ag coordination number decreases with the decrease of the sizes of Ag NPs. When Ag atoms are dispersed atomically on HMO, the Fourier transform (FT) amplitude due to the Ag–Ag bonds disappears. The first shell in the FT spectrum of Ag_1/HMO with a distance of ~2.33 Å is assigned to the Ag–O bonds with a coordination number of 4, indicating that the isolated Ag atoms are anchored onto the HMO surface to form AgO_4 motifs.[15] Malta *et al.* even performed *in situ* X-ray absorption spectroscopy experiments to definitively show that highly active catalysts comprise single-site cationic Au entities whose activity correlates with the ratio of Au(I) : Au(III) present,[78] thus providing a new way to investigate the nature of CASs under operating conditions.

IR spectroscopy may also be used to distinguish and quantify single metal atoms from metal NPs. In the late 1970s, Yates and co-workers detected the presence of single Rh atomic species in their highly dispersed Rh catalysts *via* IR spectroscopy.[79] Similarly, some recent work also utilized IR spectroscopy to differentiate and quantify the fraction of Rh single atoms and Rh nanoparticles.[80,81] Ding *et al.* also used CO as a probe molecule and assigned the IR bands centered at 2115 cm^{-1} and 2070–2090 cm^{-1} to CO adsorbed on Pt single atoms and Pt NPs, respectively (Fig. 6).[82] Hence, it is possible to compare the oxidation activity of CO adsorbed at different sites and investigate the active species in supported-Pt catalyzed CO oxidation.[82] However, it may not be suitable for all the metals to use CO as a probe molecule due to the weak CO adsorption ability of some metals. Thus, probe molecules should be carefully chosen for given SACs.

In any case, suitable characterization tools should be selected according to the operating conditions of various instruments and the nature of SACs. Moreover, it is effective to combine state-of-the-art experimental techniques and advanced modelling and simulation methods in computational

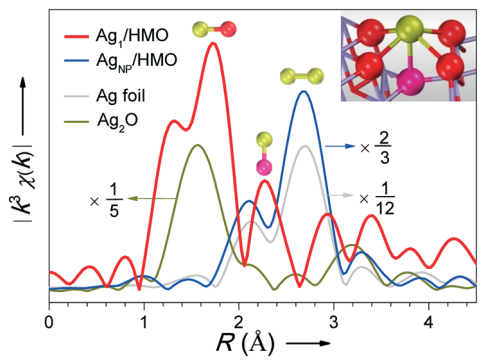

Fig. 5 Ag K-edge $\chi(R)$ k^3-weighted FT EXAFS spectra of the Ag atoms at the initial and final states during the thermal surface-mediated diffusion process of Ag_{NP}/HMO, and two reference samples of Ag foil and Ag_2O. Inset model: an isolated Ag atom anchored on the five-fold oxygen-terminated cavity of the HMO(110) surface. Yellow, red, pink and purple balls represent Ag, O with sp^3 hybridization, O with sp^2 hybridization, and Mn atoms, respectively. Reprinted with permission from ref. 69.

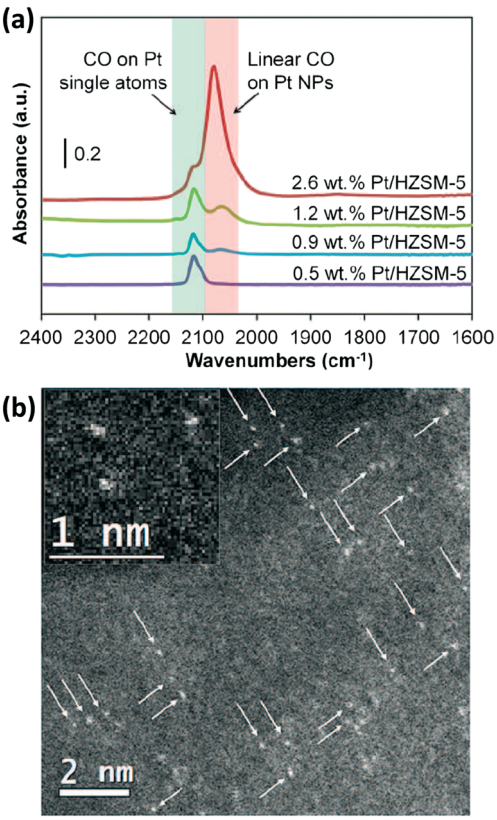

Fig. 6 (a) IR spectra of CO adsorbed on different Pt/HZSM-5 after the desorption processes. (b) HAADF image of 0.6 wt% Pt/SiO_2 (Al-doped) with magnified image inserted and arrows to mark the single atoms. Reproduced with permission from ref. 82.

chemistry in order to obtain the detailed structure of SACs. For example, Kwak *et al.* used a combination of solid-state magic-angle spinning nuclear magnetic resonance spectroscopy, STEM, and DFT calculations to find that coordinatively unsaturated pentacoordinate Al^{3+} centers were the anchoring sites for Pt atoms.[67] There is still a big room to develop a new tool with high temporal and spatial resolution for characterizing SACs, especially under reaction conditions.

4. Stability of single-atom catalysts

Stability of SACs is an important factor that often hinders the application of SACs. Due to the high surface-free energy and the low coordination number of single atoms, SACs always sinter or ripen with time, converting to their thermodynamically preferred state: fewer and larger particles.[67,83] Sintering leads to the loss of activity or selectivity, mainly through a decrease in the number of exposed metal atoms, but also through a change of the electronic properties of the metal atoms. The sintering of supported metal catalysts has been intensively studied in recent years.[75,84–91]

4.1. Thermal stability of single-atom catalysts

The sintering of supported metal NPs generally occurs by two mechanisms: coalescence and Ostwald ripening.[84,85] Coalescence occurs when two clusters touch or collide and merge to form one bigger cluster, which can occur for a high density of clusters. In the Ostwald ripening mechanism, individual metal atoms leave a smaller metal particle and diffuse around on the support surfaces until they join a bigger metal particle, leading to the growth of bigger particles at the expense of smaller ones.

Three factors that may affect the sintering process have been proposed: (i) metal effect, including the size of the NPs and the nature of the metal; (ii) support effect; (iii) metal–support interactions. Aydin *et al.* prepared MgO-supported catalysts with different metal clusters, Ir, Pt, and Au. After the same treatment in H_2 and in the electron beam, the majority of the Ir species were nanoclusters about 1 nm in diameter, while the diameters of Au and Pt NPs range from 2 to 5 nm, indicating that the sintering behavior of different metals differs, and that Ir may be an intrinsically sinter-resistant metal.[75] Campbell's group determined the variation of the heat of adsorption with changing particle size, and found that small particles have a much lower heat of adsorption than larger particles, leading to the lower onset temperature for Ostwald ripening.[84,86] Furthermore, they measured the energies of Ag atoms in Ag NPs supported on different cerium and magnesium oxide surfaces, and found that Ag NPs of any given size below 1000 atoms had much higher stability on reduced CeO_2(111) than on MgO(111). This effect was found to be a result of strong bonding to both defects and CeO_2(111) terraces.[88] Single metal atoms are in principle easier to aggregate than metal NPs, and thus strong metal–support interactions (SMSI) should be vital for the stability of SACs.

As proposed by Tauster and co-workers in the late 1970s,[92] SMSI has been extensively studied and widely used to explain the stability and activity of catalysts. For SACs, single metal atoms interact with the metal oxide either through direct M_a–M_s bonding or through the formation of M_a–$(O–M_s)_n$, where M_a and M_s represent the supported active metal atoms and the metal cations of supports, respectively, and n is a positive integer (often $1 < n < 9$). Thus, SMSI is often associated with the number (n) and the strength of the bonds, and increasing the number and the strength of the bonds will strengthen the SMSI, resulting in higher stability of SACs. For example, phosphomolybdic acid (which furnishes a range of coordination sites, including single corner site, bridge site, three-fold hollow site, and four-fold hollow site) was used to differentiate the ability of various sites for stabilizing SACs.[25] Experimental results combined with DFT calculation revealed that Pt atoms do indeed prefer to be on the four-fold hollow sites. Alkali ions were also used to stabilize single atoms such as Au and Pt, by increasing the –O ligands binding directly to the central metal atoms.[29,35] Jones *et al.* mixed ceria powders with Pt/Al_2O_3 and then calcined the mixture at 800 °C.[93] The Pt transferred to the ceria was trapped there to form a sinter-resistant and atomically dispersed catalyst, indicating that SMSI may be beneficial for the stability of SACs.[93]

4.2. Reaction stability of single-atom catalysts

Even though thermally stable SACs can be successfully synthesized, chemical or reaction stabilization of these surface single atoms remains to be a challenge due to the presence of oxidative or reducing reactants and high temperature under operating conditions. Reactants, such as CO, NO, H_2, and O_2, could affect or induce dramatically the sintering, disruption, and re-dispersion of supported metal particles, as well as supported single metal atoms.[94–96] For example, Parkinson's group has found that CO induced the coalescence of Pd adatoms supported on Fe_3O_4(001) surfaces at room temperature.[94] However, in the Pt/Fe_3O_4 system, CO plays a dual role: CO-induced mobility leads to the agglomeration of Pt into subnanometer clusters, and the presence of CO stabilizes the smallest clusters against decay.[95] The strong interaction between the reactant and the metal adatom is essential for reactant-assisted Ostwald ripening and induced disintegration. By DFT calculations, Li's group[90] proposed that when the adsorption of reactants on the metal adatoms is exothermic, the metal–reactant complexes becomes the dominant monomers. If not, Ostwald ripening will be promoted.

For the synthesis of a catalyst with high thermal and chemical stability, SMSI should be the essential factor. Kyriakou *et al.* anchored single Pd atoms in the lattice matrix on Cu(111) surfaces to obtain an extremely stable SAC with strong Pd–Cu bonds.[24] Zhang's group prepared a series of single-atom Co–N–C catalysts with single Co atoms strongly bonded with four pyridinic N atoms, which showed high stability for the chemoselective hydrogenation of nitroarenes

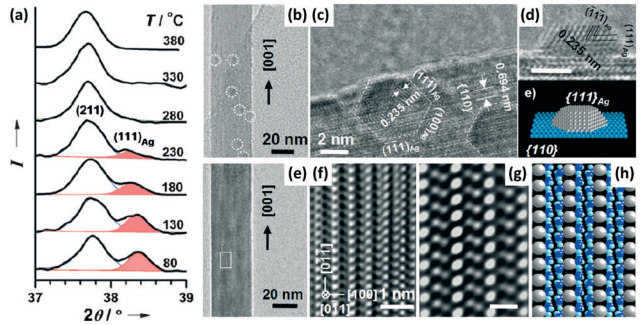

Fig. 7 (a) *In situ* XRD patterns of Ag/HMO at different temperatures. (b) TEM image of the SNP (white dotted circles) supported on a typical HMO nanorod with a [001] growth direction. (c) HRTEM image of the Ag/HMO showing a hexagonal SNP. (d) HRTEM image of the Ag particle of Ag/HMO. (e) TEM image and (f) HRTEM image of an Ag–HMO nanorod with a [001] growth direction, indicating the Ag atom chains. (g) Auto-correlation function analysis and (h) simulated images of the panel (f) showing Ag single-atom chains. Scale bar: 0.5 nm in the panel (g). Reproduced with permission from ref. 34.

and aerobic oxidative cross-coupling of primary and secondary alcohols.[49,97] They also developed a highly stable supported single Ru catalyst in a polar protic liquid phase under hydrothermal conditions.[98] We designed single-atom Ag catalyst with excellent thermal and chemical stability by initially depositing Ag NPs on HMO surfaces, and then annealing the sample at 500 °C in air. Thus, Ag atoms can diffuse into the HMO tunnels to form a Ag atom chain inside, which exposed the end atoms on the surfaces to achieve SAC (Fig. 7).[34,51] Such a single-atom Ag catalyst with four strong Ag–O bonds and one Ag–Ag bond shows high thermal stability at a temperature as high as 500 °C, and when part of Ag–O bonds were broken during reactions such as HCHO oxidation, strong Ag–Ag bond can maintain the exposed single Ag atoms to be at a steady state, thereby surviving after high-temperature annealing or chemical reactions. With SMSI, single-atom Co, Rh, and Fe catalysts exhibit excellent performance stability in a variety of reactions, such as hydroformylation, electrochemical hydrogen production, oxidation, reduction, and photocatalysis.[37,99–102]

5. Conclusions and outlook

SACs, as a kind of frontier catalysts, have attracted widespread attention and been extensively studied in recent years. However, examples on the successful preparation of SACs are still limited in number. One has to choose the support, metal, and preparation methods/conditions very carefully to obtain SACs because supported metal atoms typically tend to agglomerate to form nanoparticles, not to mention that the preparation and catalytic reaction often entail high-temperature treatment or operation. In addition, the characterization of the prepared catalysts should be carefully conducted to make sure that the supposedly formed SACs are indeed so.

Even with the difficulties associated with the preparation, characterization, and stabilization of SACs, great progress has been made in this research direction. Several types of supports can be used to fabricate SACs, *i.e.*, support surfaces with unsaturated coordinated atoms, support surfaces with defects, and support surfaces with excess O atoms. In particular, the terminated oxygen atoms of HMO(110) or (001) surfaces can anchor individual metal atoms with a proper diameter such as Ag, and the HMO tunnels could also encapsulate the individual Ag atoms.

Compared with conventional supported catalysts portrayed by the dispersion of metal nanoparticles on supports, SACs have advantages associated with maximum atom efficiency and unique catalytic properties, and the development of SACs provides new opportunities for us to identify the nature of catalytically active sites and elucidate the reaction mechanisms. However, those are not easy tasks.

For future research, it is desirable to develop more SACs with high thermal/chemical stability and excellent catalytic performance, characterize their structural details, carry out relevant experimental/theoretical studies to elucidate the nature of active sites and reaction mechanism, and demonstrate their applications in a wide range of useful catalytic reactions for energy generation, water purification, gas emission control, and production of chemicals. Research along this direction should be very interesting and fruitful.

Conflicts of interest

There are no conflicts of interest to declare.

Acknowledgements

This work was financially supported by the NSFC (21477023) and the STCSM (14JC1400400).

Notes and references

1 J. M. Thomas, R. Raja and D. W. Lewis, *Angew. Chem., Int. Ed.*, 2005, **44**, 6456–6482.
2 M. Flytzani-Stephanopoulos and B. C. Gates, *Annu. Rev. Chem. Biomol. Eng.*, 2012, **3**, 545–574.
3 X. Yang, A. Wang, B. Qiao, J. Li, J. Liu and T. Zhang, *Acc. Chem. Res.*, 2013, **46**, 1740–1748.
4 M. Flytzani-Stephanopoulos, *Acc. Chem. Res.*, 2014, **47**, 783–792.
5 S. Liang, C. Hao and Y. Shi, *ChemCatChem*, 2015, **7**, 2559–2567.
6 J. Liu, *ACS Catal.*, 2017, **7**, 34–59.
7 J. M. Thomas, *Angew. Chem., Int. Ed. Engl.*, 1988, **27**, 1673–1691.
8 S. Abbet, A. Sanchez, U. Heiz, W. D. Schneider, A. M. Ferrari, G. Pacchioni and N. Rösch, *J. Am. Chem. Soc.*, 2000, **122**, 3453–3457.
9 D. K. Böhme and H. Schwarz, *Angew. Chem., Int. Ed.*, 2005, **44**, 2336–2354.
10 B. Qiao, A. Wang, X. Yang, L. F. Allard, Z. Jiang, Y. Cui, J. Liu, J. Li and T. Zhang, *Nat. Chem.*, 2011, **3**, 634–641.

11 J. M. Thomas, Z. Saghi and P. L. Gai, *Top. Catal.*, 2011, **54**, 588–594.
12 T. Fujitani and I. Nakamura, *Angew. Chem., Int. Ed.*, 2011, **50**, 10144–10147.
13 M. Shekhar, J. Wang, W. Lee, W. D. Williams, S. M. Kim, E. A. Stach, J. T. Miller, W. N. Delgass and F. H. Ribeiro, *J. Am. Chem. Soc.*, 2012, **134**, 4700–4708.
14 M. Cargnello, V. V. T. Doan-Nguyen, T. R. Gordon, R. E. Diaz, E. A. Stach, R. J. Gorte, P. Fornasiero and C. B. Murray, *Science*, 2013, **341**, 771–773.
15 Y. Chen, Z. Huang, M. Zhou, P. Hu, C. Du, L. Kong, J. Chen and X. Tang, *Chem. Commun.*, 2016, **52**, 9996–9999.
16 S. F. Hackett, R. M. Brydson, M. H. Gass, I. Harvey, A. D. Newman, K. Wilson and A. F. Lee, *Angew. Chem., Int. Ed.*, 2007, **46**, 8593–8596.
17 J. Liu, Y. Wang and J. Li, *J. Am. Chem. Soc.*, 2017, **139**, 6190–6199.
18 D. Deng, X. Chen, L. Yu, X. Wu, Q. Liu, Y. Liu, H. Yang, H. Tian, Y. Hu, P. Du, R. Si, J. Wang, X. Cui, H. Li, J. Xiao, T. Xu, J. Deng, F. Yang, P. N. Duchesne, P. Zhang, J. Zhou, L. Sun, J. Li, X. Pan and X. Bao, *Sci. Adv.*, 2015, **1**, e1500462.
19 Y. Chen, Z. Huang, M. Zhou, Z. Ma, J. Chen and X. Tang, *Environ. Sci. Technol.*, 2017, **51**, 2304–2311.
20 Y. Chen, G. Tian, M. Zhou, Z. Huang, C. Lu, P. Hu, J. Gao, Z. Zhang and X. Tang, *Environ. Sci. Technol.*, 2016, **50**, 5825–5831.
21 F. Xu, Z. Huang, P. Hu, Y. Chen, L. Zheng, J. Gao and X. Tang, *Chem. Commun.*, 2015, **51**, 9888–9891.
22 P. Hu, Z. Amghouz, Z. Huang, F. Xu, Y. Chen and X. Tang, *Environ. Sci. Technol.*, 2015, **49**, 2384–2390.
23 H. Wei, X. Liu, A. Wang, L. Zhang, B. Qiao, Y. Yang, Y. Huang, S. Miao, J. Liu and T. Zhang, *Nat. Commun.*, 2014, **5**, 5634.
24 G. Kyriakou, M. W. Boucher, A. D. Jewell, E. A. Lewis, T. J. Lawton, A. E. Baber, H. L. Tierney, M. Flytzani-Stephanopoulos and E. C. Sykes, *Science*, 2012, **335**, 1209–1212.
25 B. Zhang, H. Asakura, J. Zhang, J. Zhang, S. De and N. Yan, *Angew. Chem., Int. Ed.*, 2016, **55**, 8319–8323.
26 H. Yan, H. Cheng, H. Yi, Y. Lin, T. Yao, C. Wang, J. Li, S. Wei and J. Lu, *J. Am. Chem. Soc.*, 2015, **137**, 10484–10487.
27 Q. Fu, H. Saltsburg and M. Flytzani-Stephanopoulos, *Science*, 2003, **301**, 935–938.
28 Y. Zhai, D. Pierre, R. Si, W. Deng, P. Ferrin, A. U. Nilekar, G. Peng, J. A. Herron, D. C. Bell, H. Saltsburg, M. Mavrikakis and M. Flytzani-Stephanopoulos, *Science*, 2010, **329**, 1633–1636.
29 M. Yang, J. Liu, S. Lee, B. Zugic, J. Huang, L. F. Allard and M. Flytzani-Stephanopoulos, *J. Am. Chem. Soc.*, 2015, **137**, 3470–3473.
30 C. H. Choi, M. Kim, H. C. Kwon, S. J. Cho, S. Yun, H. T. Kim, K. J. J. Mayrhofer, H. Kim and M. Choi, *Nat. Commun.*, 2016, **7**, 10922.
31 Y. Shi, C. Zhao, H. Wei, J. Guo, S. Liang, A. Wang, T. Zhang, J. Liu and T. Ma, *Adv. Mater.*, 2014, **26**, 8147–8153.
32 S. Sun, G. Zhang, N. Gauquelin, N. Chen, J. Zhou, S. Yang, W. Chen, X. Meng, D. Geng, M. N. Banis, R. Li, S. Ye, S. Knights, G. A. Botton, T. K. Sham and X. Sun, *Sci. Rep.*, 2013, **3**, 1775.
33 X. Zhang, J. Guo, P. Guan, C. Liu, H. Huang, F. Xue, X. Dong, S. J. Pennycook and M. F. Chisholm, *Nat. Commun.*, 2013, **4**, 1924.
34 Z. Huang, X. Gu, Q. Cao, P. Hu, J. Hao, J. Li and X. Tang, *Angew. Chem., Int. Ed.*, 2012, **51**, 4198–4203.
35 M. Yang, S. Li, Y. Wang, J. A. Herron, Y. Xu, M. Mavrikakis, L. F. Allard, S. Lee, J. Huang and M. Flytzani-Stephanopoulos, *Science*, 2014, **346**, 1498–1501.
36 S. Zhang, L. Nguyen, J. Liang, J. Shan, J. Liu, A. I. Frenkel, A. Patlolla, W. Huang, J. Li and F. Tao, *Nat. Commun.*, 2015, **6**, 7938.
37 L. Wang, W. Zhang, S. Wang, Z. Gao, Z. Luo, X. Wang, R. Zeng, A. Li, H. Li, M. Wang, X. Zheng, J. Zhu, W. Zhang, C. Ma, R. Si and J. Zeng, *Nat. Commun.*, 2016, **7**, 14036.
38 H. S. Taylor, *Proc. R. Soc. London, Ser. A*, 1925, **108**, 105–111.
39 A. Bruix, J. A. Rodriguez, P. J. Ramirez, S. D. Senanayake, J. Evans, J. B. Park, D. Stacchiola, P. Liu, J. Hrbek and F. Illas, *J. Am. Chem. Soc.*, 2012, **134**, 8968–8974.
40 C. T. Campbell, *Nat. Chem.*, 2012, **4**, 597–598.
41 T. Zambelli, J. Wintterlin, J. Trost and G. Ertl, *Science*, 1996, **273**, 1688–1690.
42 M. Valden, X. Lai and D. W. Goodman, *Science*, 1998, **281**, 1647–1650.
43 O. Lopez-Acevedo, K. A. Kacprzak, J. Akola and H. Häkkinen, *Nat. Chem.*, 2010, **2**, 329–334.
44 W. A. de Heer, *Rev. Mod. Phys.*, 1993, **65**, 611–676.
45 S. Dahl, A. Logadottir, R. C. Egeberg, J. H. Larsen, I. Chorkendorff, E. Törnqvist and J. K. Nøskov, *Phys. Rev. Lett.*, 1999, **83**, 1814–1817.
46 J. K. Nøskov, T. Bligaard, B. Hvolbæk, F. Abild-Pedersen, I. Chorkendorff and C. H. Christensen, *Chem. Soc. Rev.*, 2008, **37**, 2163–2171.
47 R. Imbihl and G. Ertl, *Chem. Rev.*, 1995, **95**, 697–733.
48 M. Yang, L. F. Allard and M. Flytzani-Stephanopoulos, *J. Am. Chem. Soc.*, 2013, **135**, 3768–3771.
49 L. Zhang, A. Wang, W. Wang, Y. Huang, X. Liu, S. Miao, J. Liu and T. Zhang, *ACS Catal.*, 2015, **5**, 6563–6572.
50 H. Zhang, J. Wei, J. Dong, G. Liu, L. Shi, P. An, G. Zhao, J. Kong, X. Wang, X. Meng, J. Zhang and J. Ye, *Angew. Chem.*, 2016, **128**, 14522–14526.
51 P. Hu, Z. Huang, Z. Amghouz, M. Makkee, F. Xu, F. Kapteijn, A. Dikhtiarenko, Y. Chen, X. Gu and X. Tang, *Angew. Chem., Int. Ed.*, 2014, **53**, 3418–3421.
52 Y. Chen, J. Gao, Z. Huang, M. Zhou, J. Xiao, C. Li, Z. Ma, J. Chen and X. Tang, *Environ. Sci. Technol.*, 2017, **51**, 7084–7090.
53 L. Wang, H. Li, W. Zhang, X. Zhao, J. Qiu, A. Li, X. Zheng, Z. Hu, R. Si and J. Zeng, *Angew. Chem., Int. Ed.*, 2017, **56**, 4712–4718.
54 J. Liang, J. Lin, X. Yang, A. Wang, B. Qiao, J. Liu, T. Zhang and J. Li, *J. Phys. Chem. C*, 2014, **118**, 21945–21951.

55 M. Moses-DeBusk, M. Yoon, L. Allard, D. Mullins, Z. Wu, X. Yang, G. Veith, G. Stocks and C. K. Narula, *J. Am. Chem. Soc.*, 2013, **135**, 12634–12645.
56 R. Zhang, T. H. Lee, B. Yu, C. Stampfl and A. Soon, *Phys. Chem. Chem. Phys.*, 2012, **14**, 16552–16557.
57 W. Ding, X. Gu, H. Su and W. Li, *J. Phys. Chem. C*, 2014, **118**, 12216–12223.
58 U. Heiz, A. Sanchez, S. Abbet and W.-D. Schneider, *J. Am. Chem. Soc.*, 1999, **121**, 3214–3217.
59 S. Vajda and M. G. White, *ACS Catal.*, 2015, **5**, 7152–7176.
60 W. E. Kaden, T. Wu, W. A. Kunkel and S. L. Anderson, *Science*, 2009, **326**, 826–829.
61 J. Lin, B. Qiao, J. Liu, Y. Huang, A. Wang, L. Li, W. Zhang, L. F. Allard, X. Wang and T. Zhang, *Angew. Chem., Int. Ed.*, 2012, **51**, 2920–2924.
62 B. Qiao, A. Wang, T. Zhang and J. Liu, *Microsc. Microanal.*, 2015, **21**, 1733–1734.
63 X. Gu, B. Qiao, C. Huang, W. Ding, K. Sun, E. Zhan, T. Zhang, J. Liu and W. Li, *ACS Catal.*, 2014, **4**, 3886–3890.
64 B. Qiao, J. Liang, A. Wang, C. Xu, J. Li, T. Zhang and J. Liu, *Nano Res.*, 2015, **8**, 2913–2924.
65 B. Qiao, J. Liu, Y. Wang, Q. Lin, X. Liu, A. Wang, J. Li, T. Zhang and J. Liu, *ACS Catal.*, 2015, **5**, 6249–6354.
66 S. Duan, R. Wang and J. Liu, *Microsc. Microanal.*, 2015, **21**, 1729–1730.
67 J. H. Kwak, J. Hu, D. Mei, C. Yi, D. H. Kim, C. H. Peden, L. F. Allard and J. Szanyi, *Science*, 2009, **325**, 1670–1673.
68 F. Dvořák, M. FarnesiCamellone, A. Tovt, N.-D. Tran, F. R. Negreiros, M. Vorokhta, T. Skála, I. Matolínová, J. Mysliveček, V. Matolín and S. Fabris, *Nat. Commun.*, 2016, **7**, 10801.
69 Y. Chen, T. Kasama, Z. Huang, P. Hu, J. Chen, X. Liu and X. Tang, *Chem. – Eur. J.*, 2015, **21**, 17397–17402.
70 S. Wang, A. Y. Borisevich, S. N. Rashkeev, M. V. Glazoff, K. Sohlberg, S. J. Pennycook and S. T. Pantelides, *Nat. Mater.*, 2004, **3**, 143–146.
71 J. Lu, C. Aydin, N. Browning and B. C. Gates, *Angew. Chem.*, 2012, **124**, 5944–5948.
72 P. D. Nellist and S. J. Pennycook, *Science*, 1996, **274**, 413–415.
73 J. Liu, *ChemCatChem*, 2011, **3**, 934–948.
74 P. A. Midgley, M. Weyland, J. M. Thomas and B. F. Johnson, *Chem. Commun.*, 2001, 907–908.
75 C. Aydin, J. Lu, N. D. Browning and B. C. Gate, *Angew. Chem., Int. Ed.*, 2012, **51**, 5929–5934.
76 J. C. Vickerman and I. S. Gilmore, *Surface analysis: The principal techniques*, John Wiley and Sons, New York, U.S.A, 2nd edn, 2009.
77 A. Jentys, *Phys. Chem. Chem. Phys.*, 1999, **1**, 4059–4063.
78 G. Malta, S. A. Kondrat, S. J. Freakley, C. J. Davies, L. Lu, S. Dawson, A. Thetford, E. K. Gibson, D. J. Morgan, W. Jones, P. P. Wells, P. Johnston, C. R. A. Catlow, C. J. Kiely and G. J. Hutchings, *Science*, 2017, **355**, 1399–1403.
79 Y. Yates Jr., T. S. D. Worley, T. M. Duncan and R. W. Vaughan, *J. Chem. Phys.*, 1979, **70**, 1225–1230.
80 J. C. Matsubu, V. N. Yang and P. Christopher, *J. Am. Chem. Soc.*, 2015, **137**, 3076–3084.
81 R. Lang, T. Li, D. Matsumura, S. Miao, Y. Ren, Y. T. Cui, Y. Tan, B. Qiao, L. Li, A. Wang, X. Wang and T. Zhang, *Angew. Chem., Int. Ed.*, 2016, **55**, 16054–16058.
82 K. Ding, A. Gulec, A. M. Johnson, N. M. Schweitzer, G. D. Stucky, L. D. Marks and P. C. Stair, *Science*, 2015, **350**, 189–192.
83 Y.-T. Kim, K. Ohshima, K. Higashimine, T. Uruga, M. Takata, H. Suematsu and T. Mitani, *Angew. Chem., Int. Ed.*, 2006, **45**, 407–411.
84 C. T. Campbell, S. C. Parker and D. E. Starr, *Science*, 2002, **298**, 811–814.
85 M. Bowker, *Nature*, 2002, **1**, 205–206.
86 S. C. Parker and C. T. Campbell, *Phys. Rev. B*, 2007, **75**, 035430.
87 M. A. Newton, C. Belver-Coldeira, A. Martínez-Arias and M. Fernández-García, *Nat. Mater.*, 2007, **6**, 528–532.
88 J. A. Farmer and C. T. Campbell, *Science*, 2010, **329**, 933–936.
89 S. R. Challa, A. T. Delariva, T. W. Hansen, S. Helveg, J. Sehested, P. L. Hansen, F. Garzon and A. K. Datye, *J. Am. Chem. Soc.*, 2011, **133**, 20672–20675.
90 R. Ouyang, J. Liu and W. Li, *J. Am. Chem. Soc.*, 2013, **135**, 1760–1771.
91 C. T. Campbell and J. R. V. Sellers, *Faraday Discuss.*, 2013, **162**, 9–30.
92 S. J. Tauster, S. C. Fung and R. L. Garten, *J. Am. Chem. Soc.*, 1978, **78**, 170–175.
93 J. Jones, H. Xiong, A. T. DeLaRiva, E. J. Peterson, H. Pham, S. R. Challa, G. Qi, S. Oh, M. H. Wiebenga, X. I. P. Hernández, Y. Wang and A. K. Datye, *Science*, 2016, **353**, 150–154.
94 G. S. Parkinson, Z. Novotny, G. Argentero, M. Schmid, J. Pavelec, R. Kosak, P. Blaha and U. Diebold, *Nat. Mater.*, 2013, **12**, 724–728.
95 R. Bliem, J. E. S. van der Hoeven, J. Hulva, J. Pavelec, O. Gamba, P. E. de Jongh, M. Schmid, P. Blaha, U. Diebold and G. S. Parkinson, *Proc. Natl. Acad. Sci. U. S. A.*, 2016, **113**, 8921–8926.
96 S. Horch, H. T. Lorensen, S. Helveg, E. Lægsgaard, I. Stensgaard, K. W. Jacobsen, J. K. Nørskov and F. Besenbacher, *Nature*, 1999, **398**, 134–136.
97 W. Liu, L. Zhang, W. Yan, X. Liu, X. Yang, S. Miao, W. Wang, A. Wang and T. Zhang, *Chem. Sci.*, 2016, **7**, 5758–5764.
98 W. Cao, W. Luo, H. Ge, Y. Su, A. Wang and T. Zhang, *Green Chem.*, 2017, **19**, 2201–2211.
99 G. Liu, A. W. Robertson, M. M.-J. Li, W. C. H. Kuo, M. T. Darby, M. H. Muhieddine, Y.-C. Lin, K. Suenaga, M. Stamatakis, J. H. Warner and S. C. E. Tsang, *Nat. Chem.*, 2017, DOI: 10.1038/nchem.2740.
100 H. Zhang, J. Wei, J. Dong, G. Liu, L. Shi, P. An, G. Zhao, J. Kong, X. Wang, X. Meng, J. Zhang and J. Ye, *Angew. Chem., Int. Ed.*, 2016, **55**, 14310–14314.
101 H. J. Qiu, Y. Ito, W. Cong, Y. Tan, P. Liu, A. Hirata, T. Fujita, Z. Tang and M. Chen, *Angew. Chem., Int. Ed.*, 2015, **54**, 14031–14035.
102 Y. Chen, S. Ji, Y. Wang, J. Dong, W. Chen, Z. Li, R. Shen, L. Zheng, Z. Zhuang, D. Wang and Y. Li, *Angew. Chem., Int. Ed.*, 2017, **56**, 6937–6941.

